ELSEVIER

Journal of Photochemistry and Photobiology A: Chemistry 126 (1999) 37–42

Journal of Photochemistry and Photobiology A:Chemistry

www.elsevier.nl/locate/jphotochem

Photolysis reaction mechanism of dibenzophenoneoxime hexamethylenediurethane, a new type of photobase generator

Hanshin Hwang [a], Du-Jeon Jang[a,*,1], Kyu Ho Chae [b]

[a] *Department of Chemistry and Research, Institute of Molecular Sciences, Seoul National University, Seoul 151-742, South Korea*
[b] *Department of Polymer Engineering, Chonnam National University, Chonnam 500-757, South Korea*

Received 29 March 1999; received in revised form 28 May 1999; accepted 1 June 1999

Abstract

The photochemical and photophysical phenomena of dibenzophenoneoxime hexamethylenediurethane have been investigated with laser flash photolysis to understand its participating mechanism in polymer curing reactions. Owing to the extremely short lifetimes of the first excited singlet (22 ps) and triplet (10 ns) (n, π^*) states, that the molecules undergo, with a small quantum efficiency of 10^{-4}, decarboxylation at the lowest triplet state with the rate constant of $10^6\ s^{-1}$, forming dehydrogenated iminyl and aminyl radicals. Abstracting a hydrogen atom in the time scale of 270 μs, the iminyl radical converts mainly into diphenyl-1-imine which, with being irradiated, dehydrogenates and dimerizes to yield benzophenone azine. Meanwhile, the aminyl radical abstracts H to generate benzophenoneoxime-urethanyl hexamethyleneamine, which, as a photobase, raises solution pH.

Keywords: Oxime urethane; Photolysis reaction; Photobase generator; Decarboxylation

1. Introduction

Reactive centers formed photochemically initiate polymerization so that they are an essential component in photochemical polymerization reactions. Although most active centers are radical, ionic ones are advantageous in microlithography, photoresists, and coating applications. Among ionic ones, anionic active centers have been studied recently [1–4], while cationic ones have been studied very well [5,6]. A variety of chemical systems such as o-nitrobenzoyl carbamates and urethanes [1,7,8], ammonium salts [3,9], amine complex [10], o-acyloxime [11,12], acetanilide [13,14], and oxime-urethanes [15,16] have been studied to produce free amines photochemically, which initiate anionic polymerization reactions such as curing reactions of epoxy resins.

While the reactions and practical applications of photobase generating precursors have been actively studied, detailed photolysis mechanisms are not understood yet. Carbamates of 9-fluorenone oxime derivatives are reported [17] to undergo decarboxylation to generate dehydrogenated iminyl and aminyl radicals concomitantly. The observations [18] of imine, azine, and amines as the photolysis products of oxime-urethane derivatives also support decarboxylation as the decomposition reaction and suggest dehydrogenated iminyl and aminyl radicals as reaction intermediates in the photolysis of oxime-urethane derivatives [15]. The amines generated from the photolysis of oxime-urethane groups contained in resins initiate polymer curing reactions as anionic photoinitiators [16].

This paper reports our study on the photophysics and photochemistry of dibenzophenoneoxime hexamethylenediurethane (BHU), an oxime-urethane derivative, as BHU is reported [15] to form amines upon irradiation which induce cross-linking of poly(glycidyl) methacrylate efficiently. We have investigated them by monitoring time-resolved fluorescence spectra and decay profiles as well as picosecond and microsecond transient absorption kinetic profiles in order to shed light on the photobase generating mechanism of BHU. Our results showing the time-resolved mechanism of BHU photolysis may signify that BHU is a good precursor of anionic photoinitiator for practical applications.

* Corresponding author.
E-mail address: djjang@plaza.snu.ac.kr (D.-J. Jang)
[1] Also a member of the Center for Molecular Science, Taejon 305-701, Korea.

1010-6030/99/$ – see front matter
PII: S1010-6030(99)00129-X

2. Experimental details

2.1. Materials

Preparation, purification, and identification of BHU were previously described in detail [15]. Ethanol, purchased from the Hayman, was used as received. The typical concentration of BHU was 5×10^{-4} M. Samples were at room temperature for all the measurements and, if not specified otherwise, they were fresh ethanol solutions.

2.2. Static measurement

Absorption spectral change with photolysis was monitored by measuring the absorption spectrum of a sample at scheduled intervals quickly with a spectrophotometer (Scinco, UVS2040) while irradiating the sample in a 2 mm quartz cell with 266 nm, 4 mJ pulses from a Nd: YAG laser (Quantel, YG501) run at 10 Hz. Static fluorescence and excitation spectra were measured by using a home-made fluorometer, which consists of a 75 W Xe lamp (Acton Research, XS432), 0.15 and 0.30 m monochromators (Acton Research, SpectroPro-150 and 300) and a photomultiplier tube (Acton Research, PD438).

2.3. Kinetic measurement

Fluorescence kinetic profiles and time-resolved spectra were measured by using a 10 ps streak camera (Hamamatsu, C2830) which was attached with a CCD detector (Princeton Instruments, RTE128H). Emission was collected from the front surface of the sample excitation for all the static and time-resolved fluorescence measurements. However, the wavelength-dependent variation of detector sensitivity was corrected for time-resolved fluorescence spectra but not for static ones. 30 ps excitation pulses from the same actively/passively mode-locked Nd: YAG laser were focused on sample in a 2 mm cell with the spot size of 2 mm diameter for fluorescence and transient absorption kinetic measurements. Picosecond transient absorption kinetic profiles were obtained by comparing laser dye emission kinetic profiles seen by the streak camera, without and with sample excitation. Microsecond time-resolved transient absorption kinetic profiles and spectra were obtained by monitoring transmittance changes, made by sample excitation pulses, of a 300 W Xe lamp (Schoeffel, LPS255) beam passing through a sample. The probe beam, wavelength-selected using two 0.25 m momochromators (Kratos, GM252), was detected with a photomultiplier tube (Hamamatsu, R928) and digitized with a 200 MHz oscilloscope (Tektronix, TDS350) which was interfaced to a 586 PC computer. The laser and the oscilloscope were triggered with variable delays by a pulse/delay generator (Stanford Research Systems, DG535). Fluorescence and transient absorption kinetic time constants were extracted by fitting measured kinetic profiles to computer simulated kinetic curves convoluted with the instrument temporal response functions.

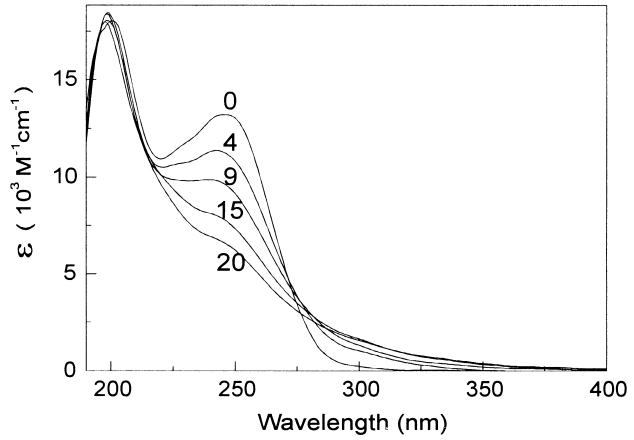

Fig. 1. Absorption spectral change of a 5×10^{-4} M BHU ethanol solution with photolysis by 4 mJ laser pulses of 266 nm at 10 Hz. The irradiation times in min are indicated near the respective spectra.

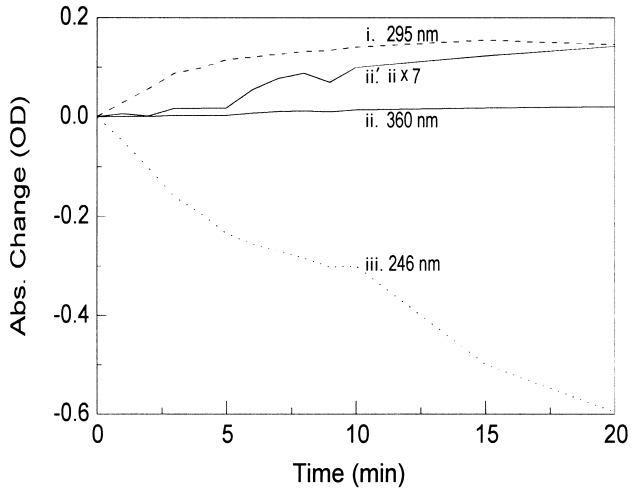

Fig. 2. Absorbance changes at three wavelengths of a BHU ethanol solution with irradiation time. The profile ii was multiplied seven times to yield the ii′ one.

3. Results and discussion

Irradiation with 266 nm light changes the absorption spectrum of BHU ethanol solution gradually (Fig. 1). The absorbance at 246 nm decreases while those at 295 and 360 nm increase with irradiation. Furthermore, Fig. 2 indicates that the absorption kinetics at three monitored wavelengths are different from each other. The absorbance at 246 nm decreases monotonically with irradiation and that at 295 nm rises earlier than the absorbance at 360 nm and stays almost constant during the later irradiation time while the absorbance at 360 nm rises slowly with some time delay. Considering their different formation times and relative transition energies, temporarily we call the species forming relatively earlier and later as a fragment product (P_F) and a com-

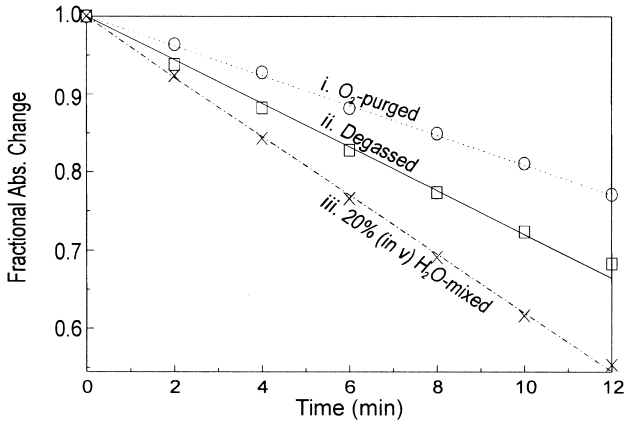

Fig. 3. Fractional absorbance changes at 246 nm of diverse BHU ethanol solutions with irradiation time.

plex product (P_C), respectively. We suggest that the species P_F forms by the photolysis of BHU and then converts into the species P_C with further absorption of light. The absorption decrease at 246 nm results from the decomposition of BHU.

The photolysis quantum efficiency of degassed sample at 266 nm has been carefully determined to be small as 10^{-4}. The photolysis efficiency reduces relatively by 27% in O_2-purged samples but enlarges by 32% in 20% (in volume) water-mixed samples (Fig. 3). The decrease in the presence of O_2 implies that the photodecomposition takes place at the lowest triplet state. The quenching of the triplet state population by the T_0 state of O_2 would cut down the photolysis efficiency. However, somewhat small (27%), rather than drastic, decrease of the photolysis efficiency implies that the (n, π^*) The T_1 state of BHU has an extremely short lifetime intrinsically in ethanol solution. The low photolysis efficiency of 10^{-4} also supports the short lifetime of the T_1 state. The increase of photolysis efficiency in water-mixed ethanol, which has a larger dielectric constant than water-free ethanol, may suggest that the dipole of BHU increases at the transition state of photolysis [19].

The fluorescence quantum efficiency of BHU in ethanol is so low that the static emission spectrum of BHU ethanol solution is almost the same as that of BHU-free ethanol. Fig. 4 shows that the low quantum efficiency is attributable to the extremely short fluorescence lifetime of BHU. Although impurity luminescence has a very small relative amplitude in picosecond kinetic profiles, its contribution is dominant in static emission spectra as a result of its much larger lifetime. To observe the fluorescence spectral contours of BHU and its photoproducts with minimal interference from impurity luminescence, we have measured time-resolved fluorescence spectra instead of static ones. Assumed that the impurity luminescence-subtracted spectra of fresh and irradiated samples are the linearly combined fluorescence spectra of reactant and products with relatively different contributions, the fluorescence spectra of BHU and its photolyzed products are deconvoluted as the solid and dotted curves in Fig. 5(b), respectively. The fluorescence spectrum of photolyzed products shows dual peaks at 340 and 470 nm while that of the reactant shows the peak at 400 nm. The fluorescence bands shifted to the blue and to the red, compared with the reactant band, are assigned to result from the species P_F and P_C, respectively.

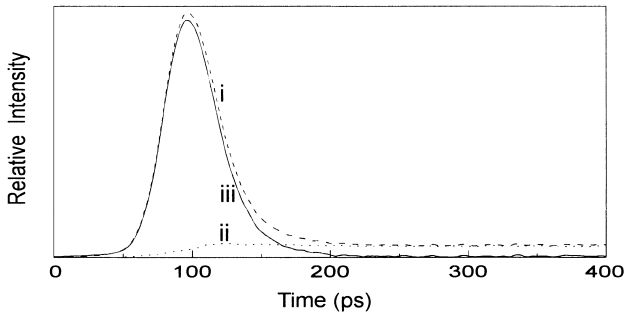

Fig. 4. Emission kinetic profiles of a BHU ethanol solution (i) and BHU-free ethanol (ii), excited at 266 nm and monitored at 450 nm. The difference (iii) is considered as the impurity luminescence-free fluorescence kinetic profile.

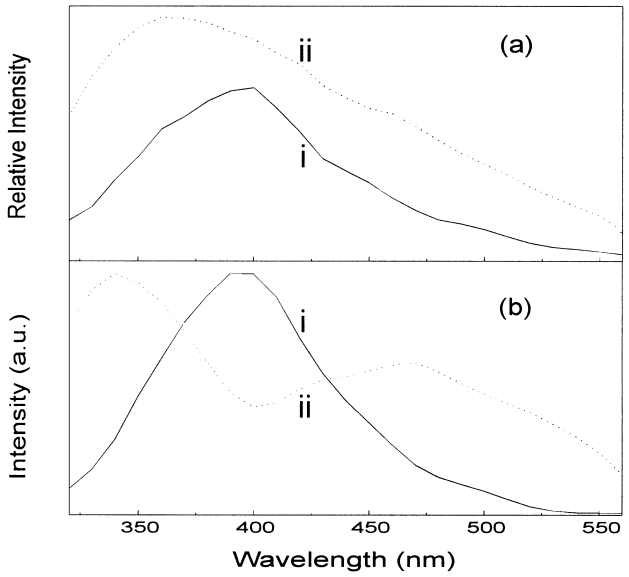

Fig. 5. Observed (a) and deconvoluted (b) time-resolved fluorescence spectra, at 20 ps after excitation, of fresh (i) and photolyzed (ii) BHU ethanol solutions.

Table 1
Decay time constants obtained from the profiles in Fig. 6

Profile	Sample	λ_{em} (nm)	Decay time constant (ps)
(a)	Fresh	400	22 (100%)
(b)	Photolyzed	340	22 (25%) + 240 (19%) + 1400 (56%)
(c)	Photolyzed	470	22 (83%) + 240 (16%) + 1400 (1%)

Fluorescence kinetic profiles near the three peak wavelengths have been examined to determine the fluorescence decay time constants of the three species BHU, P_F, and P_C as 22, 1400, and 240 ps, respectively (Fig. 6 and Table 1).

The respective static fluorescence and excitation spectra of the products P_F and P_C are observable as shown in Fig. 7,

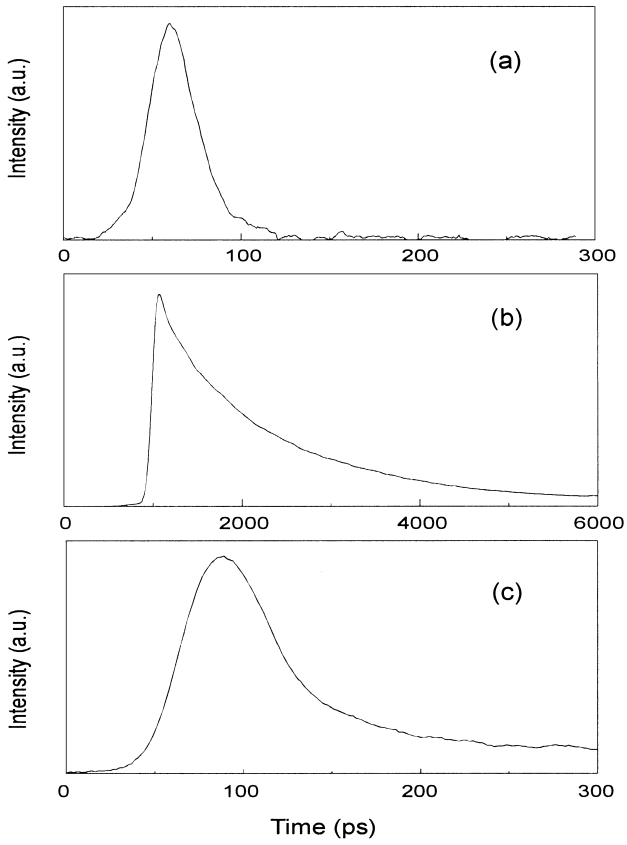

Fig. 6. Fluorescence decay kinetic profiles of a fresh BHU ethanol solution at (a) 400 nm and a photolyzed solution at (b) 340 and (c) 470 nm.

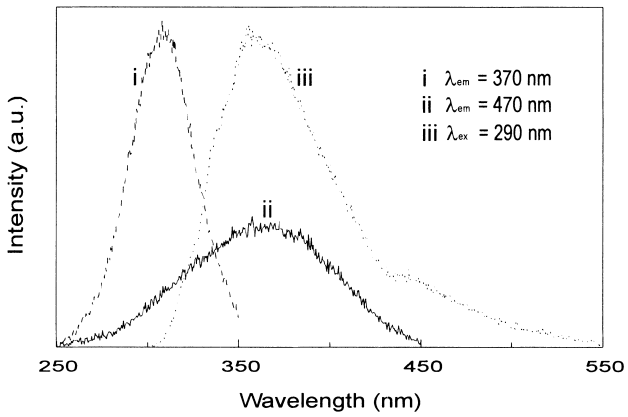

Fig. 7. Excitation (i and ii) and emission (iii) spectra of an irradiated BHU ethanol solution.

for their fluorescence lifetimes are significantly larger than that of the reactant BHU. We can notice that the static emission spectrum iii (Fig. 7) of an irradiated sample is similar to the time-resolved fluorescence spectrum of the same sample (ii in Fig. 5b), admitting that the relative intensity of P_F fluorescence is greater in the static spectrum owing to its relatively longer lifetime. The excitation spectra, obtained by monitoring the respective fluorescence bands, reveal that the lowest excitation band peaks of P_F and P_C are at 310

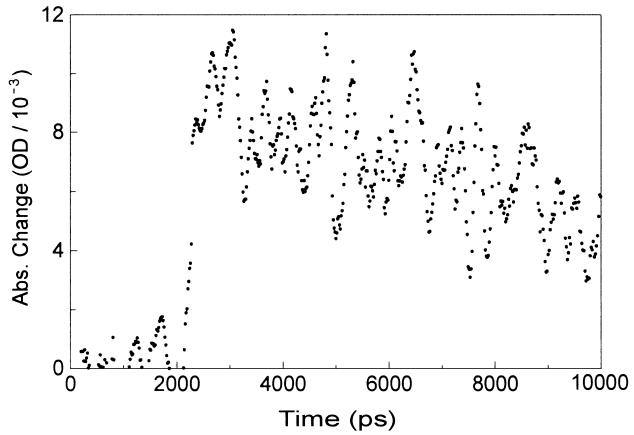

Fig. 8. Picosecond transient absorption kinetic profile of a BHU ethanol solution at 600 nm.

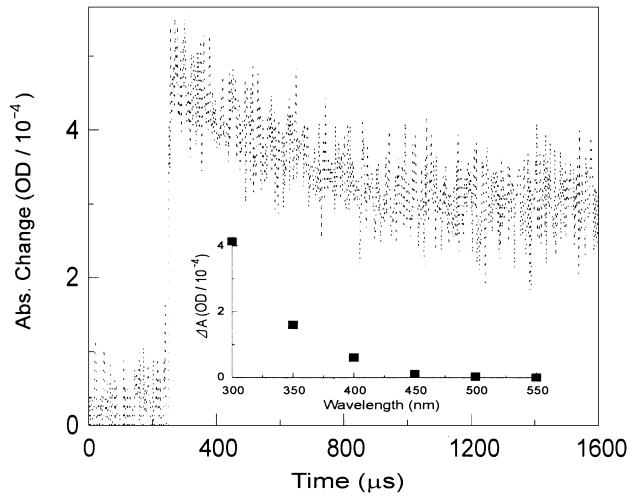

Fig. 9. Microsecond transient absorption kinetic profile of a BHU ethanol solution at 300 nm. The inset is the transient absorption spectrum of the same sample at 50 μs after laser excitation.

and 370 nm. Despite the fact that the excitation peak is usually shifted to the red from the absorption peak of a same electronic transition band, the appearance of the lowest excitation peak at 310 nm for the P_F species, whose fluorescence intensity peak at 340 nm is shifted to the blue from that of BHU at 400 nm, manifests that the absorption band of BHU with the peak at 246 nm in Fig. 1 is consequent on absorption to the (π, π^*) S_2 state rather than to the (n, π^*) S_1 state. The lowest absorption band of the reactant BHU should be shifted to the red from that of P_F and buried under the absorption bands to the (π, π^*) S_1 states of the slightly existing photolyzed products P_F and P_C that have already formed since synthesis and preparation steps.

In order to determine the kinetics and intermediates of the photolysis reaction directly rather than by means of product studies, we have examined transient absorption spectra and kinetics in the time domain of picosecond-to-second. The picosecond transient absorption kinetic profile in Fig. 8 reveals the temporal behavior of the lowest triplet state absorp-

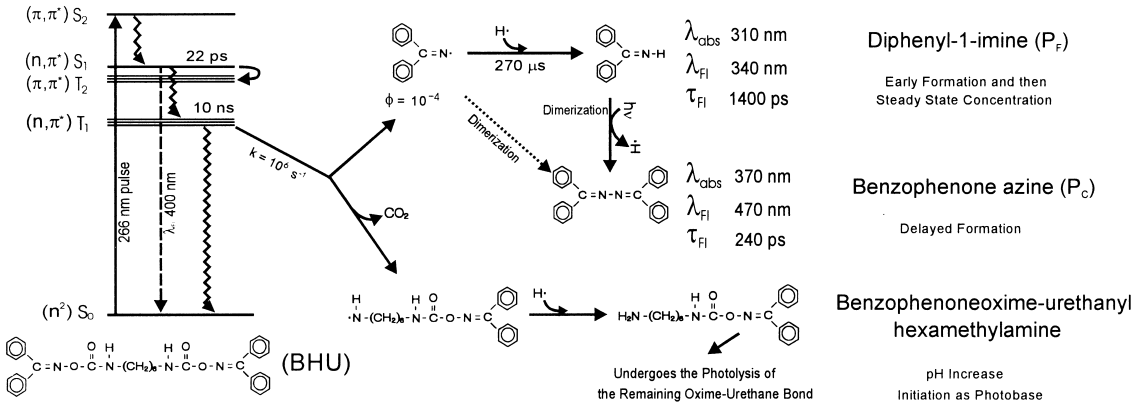

Fig. 10. Proposed reaction scheme of BHU photolysis in ethanol.

tion that rises almost instantly at our low signal-to-noise ratios and decays with the time constant of 10 ns. The kinetics suggests that following unresolvably fast internal conversion from the S_2 state, the population of the (n, π*) S_1 state undergoes a rapid intersystem crossing to the (π, π*) T_2 state that happens to lie near the S_1 state in energy. The (n, π*) T_1 state, populated immediately via internal conversion from the T_2 state, is depopulated rapidly via intersystem crossing to the S_0 ground state. The El-Sayed's rules [20,21], that the intersystem crossing transitions of S_1(n, π*)-to-*T*(π, π*) and T_1(n, π*)-to-S_0(n^2) are allowed, explain well why the S_1 and T_1 lifetimes of BHU are so short.

The T_1 transient absorbance formed upon excitation of essentially entire molecules within the excited volume is 1% of the ground state absorbance at 266 nm, and this suggests that only 1% of photoexcited molecules pass through the T_1 state during relaxation. The small intersystem crossing efficiency into the T_1 state, regardless of allowed S_1-to-T transition, is probably attributable to our excitation to the S_2 state, for an internal conversion rate increases sharply with excess excitation energy [22]. Much the reduced small transient signal in Fig. 9 suggests that again only 10^{-2} fraction of the small T_1 state population has a chance to undergo photodissociation within its decay time of 10 ns. The quantum efficiency of P_F formation, 10^{-4}, calculated from transient absorption is the same as that found from the experiment of Fig. 1. It is quite interesting to note that the overall photolysis quantum efficiency can be estimated from the product of the T_1 state transit efficiency from excitation (10^{-2}) and the dissociation efficiency from the T_1 state (10^{-2}). For the estimation of quantum efficiencies based on absorbance changes it is assumed that extinction coefficients at monitored respective wavelengths are somewhat comparable for all considered species and states. The 40% of the transient absorption in Fig. 9 decays with the time constant of 270 μs while the rest of it does not vanish within the laser pulse interval time of 0.1 s. The transient absorption spectrum measured after 50 μs of laser excitation, the inset in Fig. 9, looks like the absorption spectrum of the products in Fig. 1 in shape and it shifts somewhat to the red in energy. Considering the temporal and spectral behaviors of the two components, we propose that the decaying and nonvanishing components are attributable to a reaction intermediate and the product P_F, respectively.

BHU undergoes decomposition at the lowest triplet state. As 1% of the T_1 state population undergoes decomposition in the triplet state lifetime of 10 ns, the rate constant of BHU photodissociation is estimated as $10^6\ s^{-1}$. Considering the previous photolysis results [17] of oxime-urethane derivatives, we believe that decarboxylation occurs to give birth to dehydrogenated iminyl and aminyl radicals as photolysis intermediates. However, reported decarboxylation rate constants [23,24] are at least an order of magnitude greater than our observed photodissociation rate constant of BHU, notwithstanding that the reported species need to break a single bond while BHU needs to break two bonds if decarboxylation takes place. Although we cannot exclude the possibility of decarboxylation as the primary photodecomposition process completely, considering the decomposition rate constant and character of oxime-urethane bond, we suggest that the homolytic cleavage of the N–O bond arises first, producing dehydrogenated iminyl and carbonate radical pair as the primary intermediates.

The transient absorption with the decay time of 270 μs is the ground state absorption of the iminyl radical. The iminyl radical abstracts a hydrogen in the time scale of 270 μs to transform into diphenyl-1-imine which we called P_F. If the radical has a chance to encounter the same type of the radical within its lifetime, it may undergo, instead of hydrogen abstraction, direct dimerization promptly to produce benzophenone azine, which we called P_C. However, the early formation and then steady state concentration of the imine and the delayed formation of the azine with continuous photolysis indicate that the direct dimerization of the iminyl radical is a rather minor process for the formation of the azine, compared with the indirect dimerization of the imine after dehyrogenation upon absorption of a photon. Since the lowest absorption band spectra of the carbonate radical and its

decarboxylated dehydrogenated aminyl radical are expected to be the same as that of BHU, we cannot monitor their transient absorption spectra. However, we think that the aminyl radical, generated from the immediately followed decarboxylation of the primarily formed carbonate radical intermediate, undergoes hydrogen abstraction in much the same time scale of the hydrogen abstraction time of the iminyl radical, yielding benzophenoneoxime-urethanyl hexamethylamine [4,15,16]. In fact the generation of amines from BHU upon irradiation has been confirmed with IR spectroscopy and GC analysis [15]. The pH increase of BHU aqueous solution with irradiation time [15] also supports that BHU is photolyzed to produce amines. The quantum efficiency of the amine formation is also as low as 10^{-4} since the formation efficiency of the iminyl radical should be the same as that of the aminyl radical, which is expected to convert into the amine completely.

In summary Fig. 10 reveals how BHU, upon absorption of a photon, generates an amine as a photobase which can initiate curing reactions of polymers.

4. Conclusions

Followed the rapid internal conversion from the UV-excited (π, π^*) S_2 state, the (n, π^*) S_1 state of BHU is deactivated to the ground state in the time scale of 22 ps with a slight intersystem-crossing channel into the T_2 state. Again, followed immediate internal conversion from the T_2 state, the T_1 state is depopulated by intersystem crossing to the (n^2) S_0 ground state with the decay time of 10 ns. The populational fraction of 10^{-2} at the T_1 state undergoes decarboxyation to produce a dehydrogenated iminyl and aminyl radical pair, intimating that the rate constant of radical formation is $10^6\,s^{-1}$. The iminyl radical abstracts a hydrogen in 270 μs to form diphenyl-1-imine which upon absorption of a photon dehydrogenates and dimerizes to yield benzophenone azine. The aminyl radical goes through hydrogenation to transform into a photobase, benzophenoneoxime-urethanyl hexamethylamine which can initiate anionic polymerization reactions such as curing reaction. The extremely short lifetimes of the first excited singlet and triplet states make the photolysis quantum efficiency of BHU as small as 10^{-4}. The overall photolysis efficiency is determined by the T_1 state passage chance (10^{-2}) during relaxation and the dissociation possibility (10^{-2}) at the T_1 state.

Acknowledgements

This work was supported by the Hallym Academy of Sciences, Hallym University and the Basic Science Research Institute Program. KHC also acknowledges the Korea Science and Engineering Foundation (95-0502-07-01-3).

References

[1] J.F. Cameron, C.G. Willson, J.M.J. Fréchet, J. Am. Chem. Soc. 118 (1996) 12925.
[2] M. Tsunooka, in: J.C. Salomone (Ed.) Polymeric Materials Encyclopedia, vol. 7, CRC, New York, 1996, p. 5224.
[3] A. Mejiritski, A.Y. Polykarpov, A.M. Sarker, D.C. Neckers, Photochem. Photobiol. A: Chem. 108 (1997) 289.
[4] K.H. Chae, Sci. Tech. 8 (1997) 421.
[5] J.V. Crivello, in: S.P. Pappas (Ed.), UV Curing: Science and Technology, Technology Marketing, Norwark, USA, 1983; p. 23.
[6] J.V. Crivello, K.K. Dietliker, in: P.K.T Oldring (Eds.), Chemistry and Technology of UV and EB Formulation for Coatings, Inks and Paints, vol. III, SITA Technology, London, 1994, p. 327.
[7] J.F. Cameron, J.M.J. Frechet, J. Org. Chem. 55 (1990) 5919.
[8] J.F. Cameron, J.M.J. Frechet, J. Am. Chem. Soc. 113 (1991) 4303.
[9] J.E. Hanson, K.H. Jensen, N. Gargiulo, D. Motta, D.A. Pingor, A.E. Novembre, D.A. Mixon, J.M. Kometani, C. Knurek, ACS Sympo. Ser. 614 (1995) 137.
[10] C. Kutal, C.G. Willson, J. Electrochem. Soc. 134 (1987) 2280.
[11] K.H. Song, M. Tsunooka, M. Tanaka, J. Photochem. Photobiol. A: Chem. 44 (1988) 197.
[12] K.H. Song, M. Tsunooka, M. Tanaka, Macromol. Rapid Commun. 9 (1988) 519.
[13] T. Nishikubo, E. Takehara, A. Kameyama, J. Polym. Sci. Polym. Chem. 31 (1993) 3013.
[14] T. Nishikubo, E. Takehara, A. Kameyama, Polymer J. 25 (1993) 421.
[15] K.H. Chae, Macromol. Rapid Commun. 19 (1998) 1.
[16] K.H. Chae, H.B. Song, Polym. Bull. 40 (1998) 667.
[17] G. Bucher, J.C. Scaiano, R. Sinta, G. Barclay, J. Cameron, J. Am. Chem. Soc. 117 (1995) 3848.
[18] S.I. Hong, T. Kurosaki, M. Okawara, J. Polym. Sci. Polym. Chem. 10 (1972) 3405.
[19] K.J. Laidler, Chemical Kinetics, 3 ed., Harper and Row, New York, 1987 p. 185.
[20] M.A. El-Sayed, J. Chem. Phys. 38 (1963) 2834.
[21] N.J. Turro, Modern Molecular Photochemistry; Benjamin/Cummings, 1978; p. 168.
[22] N. Kanamaru, E.C. Lim, J. Chem. Phys. 62 (1975) 3252.
[23] L.J. Martínez, J.C. Scaiano, J. Am. Chem. Soc. 119 (1997) 11066.
[24] T.M. Bockman, S.M. Hubig, J.K. Kochi, J. Org. Chem. 62 (1997) 2210.